CHAPTER

2

Water Electrolysis Technologies

Pierre Millet [*], *Sergey Grigoriev* [†]

[*]University of Paris (XI), France, [†]National Research Center "Kurchatov Institute", Moscow, Russian Federation

OUTLINE

2.1 Introduction to Water Electrolysis 19
2.1.1 Brief Historical Review 19
2.1.2 Thermodynamics 20
2.1.3 Kinetics and Efficiencies 22
2.1.4 Main Water Electrolysis Technologies 22

2.2 Alkaline Water Electrolysis 25
2.2.1 Principles 25
2.2.2 Cell Components and Stack Structure 26
2.2.3 Performances 26
2.2.4 Technology Developments and Applications 26
2.2.5 Limitations, Recent Advances and Perspectives 28

2.3 Proton-Exchange Membrane Water Electrolysis 29
2.3.1 Principles 29
2.3.2 Cell Components 30
2.3.3 Performances 31
2.3.4 Technology Developments and Applications 31
2.3.5 Limitations, Recent Advances and Perspectives 32
2.3.5.1 Reduced PGM Contents 33
2.3.5.2 Non-PGM Catalysts 34
2.3.5.3 Higher Operating Current Densities 35
2.3.5.4 Higher Operating Temperature 35
2.3.5.5 Higher Pressure Operation 35
2.3.5.6 Other Cell Components 35
2.3.5.7 Extended Lifetime of Operation 36

2.4 High-Temperature Water Electrolysis 36
2.4.1 Principles 36
2.4.2 Cell Components 37
2.4.3 Performances 37
2.4.4 Technology Developments and Applications 38
2.4.5 Limitations, Recent Advances and Perspectives 39

2.5 Conclusion 39

References 40

2.1 INTRODUCTION TO WATER ELECTROLYSIS

2.1.1 Brief Historical Review

It is reported in the literature[1] that water electrolysis (the electricity-driven $H_2O \rightarrow H_2 + 1/2\,O_2$ reaction) was performed for the first time in 1800 by the English scientists William Nicholson (1753–1815) and Anthony Carlisle (1768–1842). Thus doing, they initiated the science of electrochemistry. It is also reported in the literature that the German scientist Johann Ritter repeated these experiments one month later and was the first able to collect evolving hydrogen and oxygen separately.[2]

The laws of electrolysis were discovered later and reported in 1833–1834 by the English scientist Michael Faraday. He established the quantitative relationship between the amount of electricity q passing through the electrode/electrolyte interface and the mass m of substances involved in the electrolysis (redox) process:

$$m = k_e q, \tag{2.1}$$

where $k_e = M/nF$ is the electrochemical equivalent in kg/C ≡ kg/(Amps × s); M in kg/mole is the molar mass of substance produced at the interface; n is the number of electrons involved in the electrochemical reaction; $F = 96{,}485.3$ C/mole is the Faraday's constant.

http://dx.doi.org/10.1016/B978-0-444-56352-1.00002-7

Faraday's law is a law of mass conservation and is therefore strictly verified. A practical condition is that new species formed at both interfaces (anode and cathode) are fully separated and do not spontaneously react with each other. Concerning water electrolysis, when the steady (stationary) electric current I and time period t are known, the theoretical (maximum) amount of hydrogen (or oxygen) produced can be calculated using:

$$V_{\text{theor.}} = \frac{k_e I t}{\rho} \tag{2.2}$$

where $V_{\text{theor.}}$ in m^3 is the theoretical volume of gas evolved, I in A is the total current, t in s is time; ρ in kg/m^3 is the gas density.

Although the principles of water electrolysis were discovered at the very early nineteenth century, it took almost a 100 years before electrolyzers of industrial scale were developed for hydrogen production in countries where hydropower was cheap and abundant. At that time, industrial applications were targeting chemical markets. In 1902, more than 400 industrial electrolyzers were in operation worldwide. In 1927, the Norwegian company Norsk Hydro Electrolyzers developed the first water–alkaline electrolyzer for the synthesis of ammonia and in 1939, the first 10,000 Nm^3/h H_2 plant was in operation. Later, a unit delivering 60,000 Nm^3/h H_2 was put in operation. In 1948, the first pressurized water electrolyzer was built and operated by Zdansky/Lonza. In 1966, the first solid polymer electrolyte (SPE) electrolyzer was built by General Electric Co. In 1972 and 1978, the development of solid-oxide water electrolysis (SOWE) and advanced alkaline water electrolysis was started, respectively. Over the last decades, new applications of hydrogen as an energy carrier, for example, in the storage of energy obtained from renewable energy sources, were found. Water electrolysis can be used for the regulation of electrical grids (peak shaving). The coupling of large-scale high-temperature water electrolyzers with nuclear power plants (using electrical power and waste heat of high-temperature helium reactor) is regarded as one of the key technologies for hydrogen production within the framework of hydrogen–nuclear energy. In addition, the production of hydrogen by electrolysis is suitable for systems based on renewable energy (solar, wind, surges, tides, etc.) that are not integrated into the network. In such cases, hydrogen can accumulate the energy to produce electricity and heat for the time periods when the renewable source does not produce electricity. Electrolyzers are also used in miscellaneous applications such as the analytical instruments (equipment for gas chromatographs), correction systems for water-chemistry mode of nuclear reactors, high-purity metals and alloys metallurgy, the production of high-purity materials for the electronics industry and hydrogen welding. It should finally be noted that electrolysis allows the concentration of heavy hydrogen isotopes in the liquid phase. This is one of the technologies used in the production of hydrogen isotopes. This is based on the fact that different isotopes undergo reactions at different rates. When deuterated water is electrolyzed, hydrogen evolves at a higher rate than deuterium relative to their concentrations. As a result, the deuterium to hydrogen ratio increases in the remaining water.[3]

2.1.2 Thermodynamics

In standard conditions (298 K, 1 bar), the water splitting reaction is as follows:

$$H_2O_{(l)} \rightarrow H_{2(g)} + \frac{1}{2}O_{2(g)} \tag{2.3}$$

Assuming that the chemical reaction is performed along a reversible path under isothermal conditions, then:

$$\Delta G(T) = \Delta H(T) - T\Delta S(T) \tag{2.4}$$

where $\Delta H(T)$ in J/mol is the enthalpy change associated with reaction (a); $\Delta H(T)$ is positive up to $\approx$2250 °C (the water splitting reaction is endothermic); $\Delta H(T)$ is the total amount of energy that must be supplied to the electrolysis cell to dissociate water into H_2 and O_2. $\Delta S(T)$ in J/mol/K is the entropy change; $\Delta S(T)$ is positive because 1 mol of water dissociates into 1.5 mol of gases. T in K is the absolute temperature. $T\Delta S(T)$ is positive. $\Delta G(T)$ in J/mol is the Gibbs free energy change; $\Delta G(T)$ is positive (reaction (a) is a nonspontaneous process) up to $\approx$2250 °C because over this temperature range, the enthalpy term is predominant over the entropic change. $\Delta G(T)$ represents the amount of electricity that must be supplied to the electrolysis cell in addition to the $T\Delta S(T)$ amount of heat to dissociate water. In standard conditions (25 °C), $\Delta G^0 = 237.23$ kJ/mol (2.94 kWh/Nm^3 H_2), $\Delta H^0 = 285.83$ kJ/mol (3.54 kWh/Nm^3 H_2), $\Delta S^0 = 163.09$ J/mol/K.

The electrolysis of water vapor is as follows:

$$H_2O_{(g)} \rightarrow H_{2(g)} + \frac{1}{2}O_{2(g)} \tag{2.5}$$

For the electrolysis of water vapor, $\Delta G^0 = 228.61$ kJ/mol (2.84 kWh/Nm^3 H_2), $\Delta H^0 = 241.81$ kJ/mol (3.00 kWh/m^3 of hydrogen) and $\Delta S^0 = 44.32$ J/mol/K. The enthalpy difference between reactions 2.3 and 2.5 is the enthalpy of water vaporization.

The electrical work required for the electrolysis of 1 mol of water in standard conditions is:

$$\Delta G_T^0 = nFE^0 \tag{2.6}$$

where E^0 in V is the standard thermodynamic voltage (for liquid water $E^0 = 1.229$ V at 25 °C). However, it is also possible to define another electrolysis voltage,

the so-called thermoneutral voltage, which is the voltage required for water electrolysis to occur at constant temperature, without exchange of heat to the surroundings:

$$E_{TN}(T) = \frac{\Delta H(T)}{nF} \tag{2.7}$$

At temperatures less than 100 °C, $E_{TN} = \Delta H^0/2F \approx 1.48$ V and slightly depends upon pressure. When a cell voltage less than E^0 volt is applied to the electrolysis cell, nothing occurs because there is not enough energy supplied to the cell to perform the nonspontaneous reaction (3). When a cell voltage U such as $E^0 < U < E_{TN}$ is applied to the electrolysis cell, electrolysis is possible but heat is required from the surrounding. If no heat is supplied, then the temperature of the electrolysis cell will decrease. At the thermoneutral cell voltage, the water dissociation reaction will take place at constant temperature, without any exchange of heat (absorption or release) to the surroundings. At voltages above the thermoneutral voltage, the electrolysis process is exothermic and heat is released to the surroundings.

Main thermodynamic functions associated with the water splitting reaction are plotted in Fig. 2.1. Abrupt changes of ΔH and $T\Delta S$ at 373 K are due to the vaporization of liquid water into vapor.

The dimensionless term η_{TD} defined as the ratio of the Gibbs free energy change to the enthalpy change can be used to express the fraction of electrical energy required for the water splitting. Since both $\Delta G(T)$ and $\Delta H(T)$ are functions of operating temperature, η_{TD} is also a function of operating temperature:

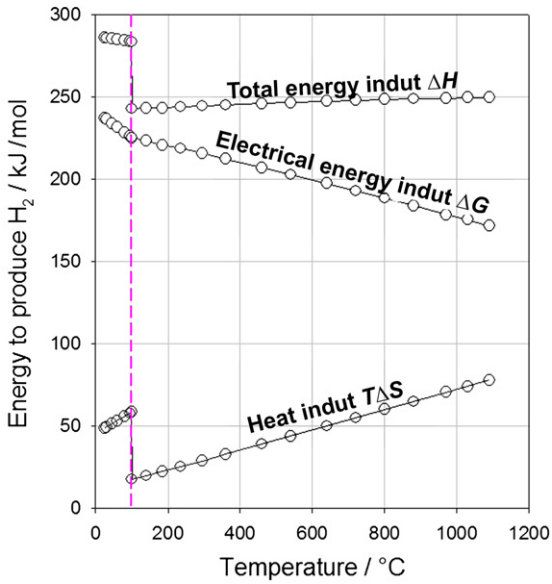

FIGURE 2.1 Temperature dependence of main thermodynamic parameters for water electrolysis. (For color version of this figure, the reader is referred to the online version of this book.)

$$\eta_{TD}(T) = \frac{\Delta G(T)}{\Delta H(T)} = \frac{E(T)}{E_{TN}(T)} \tag{2.8}$$

As can be seen from Fig. 2.1, the enthalpy of water dissociation does not change significantly with operating temperature. On the contrary, the significant change of the entropic term leads to a significant decrease in Gibbs free energy and corresponding electrolysis voltage. Therefore, the percentage η_{TD} of electricity required to split water also decreases with temperature (Table 2.1).

In the high operating temperature range (800–1000 °C), approximately two thirds of the energy required for the dissociation reaction must be supplied as electricity and one third as heat. Since the cost of the kWh of heat is usually significantly less than the cost of the kWh of electricity, the energy cost required to split water is less expensive at higher operating temperatures.

A quantitative expression of the thermodynamic cell voltage required to split water into hydrogen and oxygen can be derived from the general Nernst formula. $E(T)$ is a function of operating temperature, partial pressures of reactants and water activity in the electrolyte:

$$E = E^0 + \frac{RT}{nF}\ln\frac{P_{O_2}^{1/2}P_{H_2}}{a_{H_2O}} \tag{2.9}$$

In Eqn (2.9), E^0 is the standard value of the equilibrium cell voltage ($E^0 = \Delta G^0/2F = 1.229$ V at 25 °C for liquid water); R in J/mol/K is the absolute gas constant; T is the absolute temperature; P_{O_2} and P_{H_2} in atm are the partial pressure of the reaction products and a_{H_2O} is the activity of water in the electrolyte (close to unity in a first approximation). According to Eqn (2.9), an increase in operating pressure yields an increase in E. Nevertheless, pressurized water electrolysis is interesting because there is a need to compress hydrogen for storage and transportation, and pressurized water electrolysis can compete with electrolysis followed by mechanical compression. An additional benefit of pressurized water electrolysis is that the water vapor content of gases released from the pressurized electrolyzer is less significant than at atmospheric pressure (approximately 20–30 times lower) and the cost of the drying process is therefore reduced.

TABLE 2.1 Thermodynamic Voltage $E(T)$ and Percentage η_{TD} of Energy Required in the Form of Electricity to Split Water at Atmospheric Pressure and Different Operating Temperatures

T (°C)	25	90	800	1000
E (V)	1.229	1.176	0.978	0.920
η_{TD} (%)	83	80	66	62

2.1.3 Kinetics and Efficiencies

At equilibrium, the water splitting reaction occurs at an infinitely small rate, a situation of no practical interest. To split water into hydrogen and oxygen, the cell voltage U applied to the electrolysis cell must be significantly larger than the thermodynamic voltage in order to let a significant current density flow across the cell and reduce capital expenses. Main resistances to current flow are (1) charge transfer overvoltages at both anode/electrolyte (η_a) and cathode/electrolyte (η_c) interfaces and (2) the resistivity of the electrolyte. In industrial system, parasite ohmic losses are also encountered in electrodes and cable wiring to the electrolyzer. During water electrolysis, the anodic overvoltage is due to the charge transfer associated to the oxygen evolution reaction (OER) and the cathodic overvoltage is due to the charge transfer associated to the hydrogen evolution reaction (HER). Both terms are a function of operating current density according to the Butler–Volmer theory of charge transfer. At a current density j, the cell voltage $U(j)$ is given by:

$$U(j) = E + \eta_c(j) + \eta_a(j) + JR_{el}(j), \tag{2.10}$$

where J in A is current; R_{el} in Ohm is electrolyte resistivity.

When no mass transport limitations take place (this is usually the case in water electrolysis because of highly concentrated electrolytes and mobile charge carriers are used), values of η_c and η_a are related to the current density through the Tafel equation:

$$\eta = a + b \cdot \ln I \tag{2.11}$$

where $a = -RT/(\alpha \cdot n \cdot F) \ln i_0$ and $b = 2.303 \times RT/(\alpha \cdot n \cdot F)$, α is a transfer coefficient, i.e. the number of electrons transferred due to electrochemical reaction ($\alpha \approx 0.5$).

It can be seen from Eqn (2.11) that overvoltages decrease when the operating temperature increases. Hence, when the operating temperature of the electrolysis cell increases, less electricity is required because (1) ΔG (and η_{TD}) decrease (thermodynamic factor) and (2) the overall kinetics improves (kinetic factor). However, charge transfer overvoltages increase when the current density increases. The enthalpy efficiency of a water electrolysis cell operating at current density j and temperature T with a cell voltage $U(T,j)$ is defined as:

$$\eta_{\Delta H}(T,j) = \frac{n\,F\,E_{TN}(T,j)}{n\,F\,U(T,j)} = \frac{E_{TN}(T,j)}{U(T,j)} \tag{2.12}$$

At low current density ($j \approx 0$), $U \approx E_{TD}$ and $\eta_{\Delta H} \approx 1$. In the literature, the energy consumption per unit of mass (with units of kWh/kg) or unit of volume (with units of kWh/Nm^3) is commonly used to compare the efficiency of different electrolyzers. It should be noted, however, that both expressions are functions of the operating current density j.

Another important electrolysis cell characteristic is the current (faradic) efficiency. It is defined as the ratio of the volume of gas produced over a given time interval to the theoretical volume that should be produced during that time in accordance with Faraday's laws:

$$\eta_F = \frac{V_{actual}}{V_{theor.}} \tag{2.13}$$

Usually, $\eta_F \approx 1$ but significantly lower values are sometimes obtained. There are several reasons for such deviations, mainly (1) the energy consumption used for the electrolysis of impurities present in the electrolyte; (2) the spontaneous recombination of reaction products that are not appropriately separated during operation ($H_2 + 1/2\ O_2 \rightarrow H_2O$ in the case of water electrolysis); and (3) the formation of stray currents in the electrolysis stack when liquid electrolytes are used (alkaline process). In the alkaline and polymer electrolyte processes, the overall efficiency of the electrolysis cells is usually in the 75–85% range. In the high-temperature SOWE, even higher efficiencies (close to unity) can be reached to the high kinetics of charge transfer and to the excellent conductivity of the electrolyte at such elevated temperatures. However, the calculation of the overall efficiency of an electrolyzer should take into account the efficiency of the electrical source. The efficiency of thermal power stations is usually less than 50%, and therefore, the overall efficiency of the hydrogen production process is approximately 40%.

2.1.4 Main Water Electrolysis Technologies

There are two main experimental parameters to carry out water electrolysis: temperature and electrolyte pH. The temperature dependence of thermodynamic and enthalpy water dissociation voltage is plotted in Fig. 2.2. Whereas the enthalpy voltage remains constant almost over the entire range of practical operating temperatures (i.e. the enthalpy change ΔH does not vary significantly with operating temperature as shown in Fig. 2.1), the thermodynamic voltage significantly decreases, following the temperature dependence of the Gibbs free energy change (Fig. 2.1). Water electrolysis technologies can be classified into low-temperature processes ($T < 150\,^\circ$C), medium-temperature processes ($200\,^\circ\text{C} < T < 600\,^\circ$C) and high-temperature processes ($>600\,^\circ$C). Concerning the pH, as indicated in the previous sections, the half-cell reactions differ with the pH of the electrolyte. In acidic media, protons carry the current in the electrolyte and the following reactions take place:

$$\text{Anode}(+): H_2O(\text{liq}) \rightarrow \frac{1}{2}O_2(g) + 2H^+ + 2e^- \tag{2.14}$$

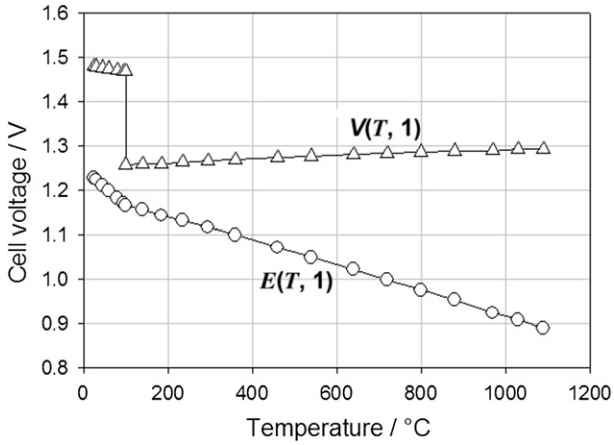

FIGURE 2.2 Thermodynamic and enthalpy water splitting voltages as a function of operating temperature.

$$\text{Cathode}\,(-): 2H^+ + 2e^- \rightarrow H_2(g) \tag{2.15}$$

$$\text{Fullreaction}: H_2O(\text{liq}) \rightarrow H_2(g) + \frac{1}{2}O_2(g) \tag{2.16}$$

Using the Nernst equation, the potential of the anode is:

$$E^+ = E^0_{H_2O/O_2} + \frac{RT}{nF} Ln \frac{\left(a^2_{H^+}\right)\left(f^{1/2}_{O_2}\right)}{a_{H_2O}} \tag{2.17}$$

At 298 K, when the pressure of oxygen is 1 bar (ideal gas), $E^+ \approx 1.23 - 0.06$ pH. Using the Nernst equation, the potential of the cathode is:

$$E^- = E^0_{H_2/H^+} + \frac{RT}{nF} Ln \frac{a^2_{H^+}}{f_{H_2}} \approx -0.06 \text{ pH} \tag{2.18}$$

At 298 K, when the pressure of hydrogen is 1 bar (ideal gas), $E^- \approx -0.06$ pH. Therefore, when the anode and cathode are immerged in the same electrolyte, the cell voltage is $E_{cell} = E^+ - E^- = 1.23$ V.

In alkaline electrolyte, different half-cell reactions take place:

$$\text{Anode}\,(+): 2OH^- \rightarrow H_2O + \frac{1}{2}O_2(g) + 2e^- \tag{2.19}$$

$$\text{Cathode}\,(-): 2H_2O + 2e^- \rightarrow H_2(g) + 2OH^- \tag{2.20}$$

$$\text{Fullreaction}: H_2O(\text{liq}) \rightarrow H_2(g) + \frac{1}{2}O_2(g) \tag{2.21}$$

Using the Nernst equation, the potential of the anode can be derived:

$$E^+ = E^0_{H_2O/O_2} + \frac{RT}{nF} Ln \frac{\left(a_{H_2O}\right)\left(f^{1/2}_{O_2}\right)}{a^2_{HO^-}} \tag{2.22}$$

At 25 °C, when the pressure of oxygen is 1 bar (ideal gas), $E^+ \approx 1.23 + \text{pKe} - 0.06$ pH. Using the Nernst equation, the potential of the cathode is:

$$E^- = E^0_{H_2O/H_2} + \frac{RT}{nF} Ln \frac{a^2_{H_2O}}{f_{H_2} a^2_{HO^-}} \tag{2.23}$$

At 25 °C, when the pressure of hydrogen is 1 bar (ideal gas), $E^- \approx \text{pKe} - 0.06$ pH.

Therefore, when the anode and cathode are immerged in the same electrolyte, the cell voltage is $E_{cell} = E^+ - E^- = 1.23$ V. From these results, it can be concluded that the thermodynamic voltage required to split water into hydrogen and oxygen is the same, whatever the pH of the electrolyte (Fig. 2.3). The only difference between alkaline and acidic water electrolysis is that the potential of each electrode is shifted along the potential axis, as a function of electrolyte pH.

Protons and hydroxyl ions are the most mobile ionic species. Concentrated solutions are required to avoid concentration overvoltages. Consequences are mostly on electrode material stability. From a historical perspective, alkaline water electrolyzers were first developed because in alkaline media, many metals are passivated and corrosion is prevented. Electrolyzers using liquid acidic electrolyte are seldom found because of severe corrosion issues. Acid water electrolysis technology developed in the late 1960s when SPEs (protons remain confined into the membrane electrolyte) became commercially available. More recently, ceramics have been used as solid electrolyte for operation at higher temperatures. For temperature above 800 °C, oxide ion (O^{2-}) conductors are preferred. In the intermediate temperature range (250–600 °C), some proton-conducting ceramics can also be used. The main features of the different water electrolysis technologies are compiled in Table 2.2.

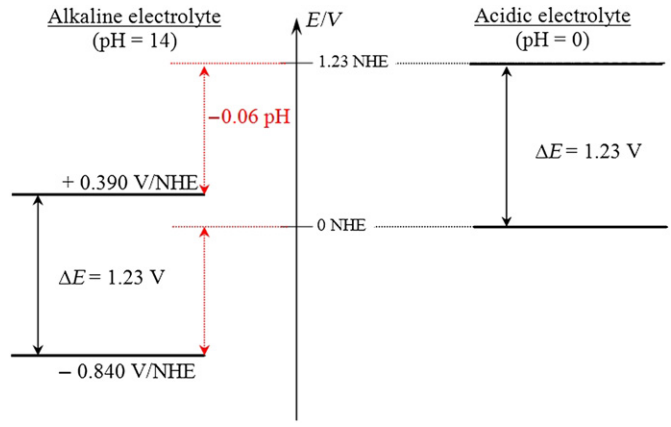

FIGURE 2.3 Electrode potential versus pH for the water splitting reaction (NHE, normal hydrogen electrode). (For color version of this figure, the reader is referred to the online version of this book.)

TABLE 2.2 Comparison of Main Water Electrolysis Technologies[4]

Technology status	Mature technology		Lab-scale, R&D	
	Alkaline	**PEM**	**Medium *T***	**Solid oxide**
T range (°C)	Ambient/120	Ambient/90	250/600	800/1000
Electrolyte/pH	25–30 wt% $(KOH)_{aq}$	PFSA*	Polymer or $Sr[Ce_xZr_{1-x}]_{0.95}$ $Yb_{0.05}O_3$,[5] $La_{0.6}Ba_{0.4}ScO_{2.8}$	Y_2O_3–ZrO_2, Sc_2O_3–ZrO_2, MgO–ZrO_2, CaO–ZrO_2
Mobile species	OH^-	H_3O^+	H_3O^+	O^{2-}
Cathode catalyst	Nickel foam/Ni-SS†	Platinum	Ni–YSZ or Ni-GDC Cermet with proton-conducting electrolyte	Ni–YSZ or Ni-GDC Cermet
Cathode carrier	Nickel foam/Ni-SS; Ni–Mo/ZrO_2–TiO_2	Carbon		
Anode catalyst	Ni_2CoO_4, La–Sr–CoO_3, Co_3O_4	Ir/Ru oxide	(La,Sr)MnO_3, (La,Sr)(Co,Fe)O_3	(La,Sr)MnO_3, (La,Sr)(Co,Fe)O_3
Anode carrier	–	–	–	Gd-doped ceria
Separator	Asbestos, PAM,‡ ZrO_2-PPS,§ NiO, Sb_2O_5-PS¶	Electrolyte membrane	Electrolyte membrane	Electrolyte membrane
Sealant	Metallic	Synthetic rubber or fluoroelastomer	Glass and vitro-ceramics	Glass and vitro-ceramics
Current distributor	Ni	Titanium		Ferritic SS (Crofer APU**)
Containment material	Nickel-plated steel	Stainless steel	Stainless steel	Stainless steel
P range (bar)	1–200	1–350 (700)	1	1–5
Conventional current density (A/cm^2)	0.2–0.5	0–3	0–0.1	0–2
Efficiency (%) (at *i* $A/cm^2/U_{cell}$ V/*T*°C)	60–80; 0.2–0.5/2.0/80	80; 1.0/1.8/90	Lab-scale tests	100; 3.6/1.48/950
Capacity (Nm^3/h)	1–500	1–230	1	1
Durability (h)	100,000	10,000–50,000	500	500–2000
H_2O specification	Liquid	$\rho > 10\,M\Omega\,cm$	Steam	Steam
Load cycling	Medium	Good	No data av.	No data av.
Stop/go cycling	Weak	Good	No data av.	Weak

* *Perfluorosulfonic acid.*
** *Auxiliary power unit.*
† *Stainless steel.*
‡ *Polysulfone-bonded polyantimonic acid.*
§ *ZrO_2-PPS—ZrO_2 on polyphenylsulfone.*
¶ *Sb_2O_5-PS—polysulfone impregnated with Sb_2O_5 polyoxide.*

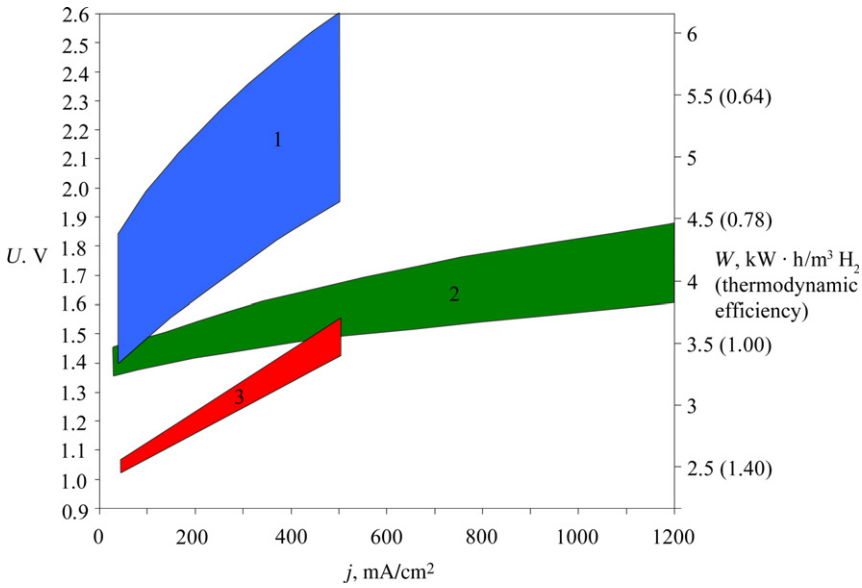

FIGURE 2.4 Polarization curves ($U-j$) and specific energy consumption of main water electrolysis technologies: 1, industrial alkaline electrolyzers (70–95 °C); 2, solid polymer electrolyzers (90–110 °C; 0–3.0 MPa); 3, high-temperature solid-oxide electrolyzers (900 °C) with additional heat supply. (For color version of this figure, the reader is referred to the online version of this book.)

The voltage–current density relationships and electricity consumption of the main water electrolysis technologies are compared in Fig. 2.4. Detailed principles and main characteristics are discussed in the next sections.

2.2 ALKALINE WATER ELECTROLYSIS

2.2.1 Principles

The general features of alkaline water electrolysis cells are pictured in Fig. 2.5.

Two metallic electrodes are immersed in a liquid electrolyte. Aqueous solutions of KOH or NaOH are usually used for that purpose. The concentration of the electrolyte solution is usually up to 40 wt% to provide maximum electrical conductivity at temperatures up to 90 °C. Specific conductivity of KOH solution is $54.3 \times 10^{-2}/\Omega/\text{cm}$ at 25 °C.[6] Water reduction takes place at the cathode of the electrolyzer according to:

$$2H_2O + 2e^- \rightarrow H_2 + 2OH^- \left(E_C^0 = -0.828\ \text{V}\right), \quad (2.24)$$

and the oxidation of hydroxyl ions takes place at the anode according to:

$$2OH^- \rightarrow \frac{1}{2}O_2 + H_2O + 2e^- \left(E_A^0 = +0.401\ \text{V}\right). \quad (2.25)$$

Only water is consumed during the process and therefore water has to be supplied to the cell to feed the reaction and maintain the concentration of the electrolyte to an optimum value. At usual operating temperature (60–80 °C), water vapor and traces of electrolyte are also carried away by gas products. On a dry basis, hydrogen purity is usually ≈99.9%.

As can be seen from Fig. 2.5, a cell separator (usually a porous and electrolyte-impregnated material) is placed between the two electrodes to avoid the spontaneous back recombination of H_2 and O_2 into water. In a gap-cell configuration, the two massive electrodes are placed face to face, allowing a small (a few mm thick) electrolyte gap between the electrodes and the separator where gaseous H_2 and O_2 are evolved. As the current density increases, gas bubbles tend to form a continuous and highly resistive film at the surface of both electrodes and as a result, operating current densities are limited to values up to a few 100 mA/cm^2. In the more-efficient zero-gap cell configuration, the two electrodes are porous and pressed against the cell separator. Thus, the interpolar distance is lower and gases are evolved at the back of the electrodes, allowing higher current density values to be reached.

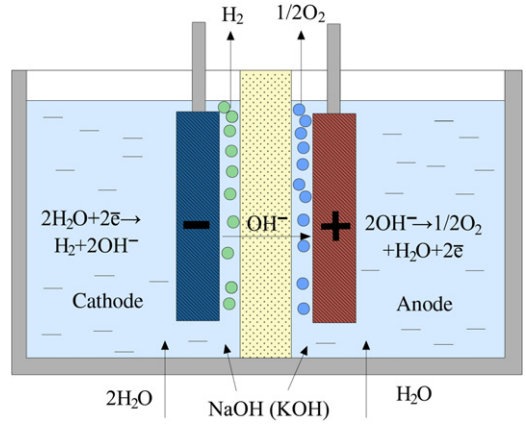

FIGURE 2.5 Schematic diagram of the alkaline electrolysis cell. (For color version of this figure, the reader is referred to the online version of this book.)

2.2.2 Cell Components and Stack Structure

Steel grids are usually used as electrode materials. In some cases, in order to improve the charge transfer kinetics, these grids are covered with a layer of porous nickel produced by leaching of zinc from the Ni–Zn alloy (Raney nickel). For several decades, asbestos (natural silicate mineral) has been used for the porous diaphragm-separating anode and cathode. But due to the toxicity of the material (the inhalation of asbestos fibers can cause lung cancer), the need for harmless materials has led to the development of a large variety of alternative solutions, in particular to the development of polymer-based composite materials.[7] It should be mentioned that the presence of a porous diaphragm generates some specific operating problems. In particular, safety issues may become critical, especially at elevated pressures, because of the possible mixing of product gases. Moreover, gas purity tends to decrease when operating pressure is raised. The advantages of alkaline water electrolysis over other water electrolysis processes are as follows: (1) relatively lower capital expenses due to the use of cheap cell materials (electrodes and separators), (2) proven technology with well-established operational costs; (3) demonstration of large capacity units; and (4) raw water can be used directly in the process without the need for specific purification procedures. On the less positive side, the quality of hydrogen (and oxygen) is quite low (hydrogen contains impurities of oxygen, water vapor with alkali) and higher hydrogen purity requires additional purification steps. Most alkaline water electrolyzers are built using a filter-press configuration. The stack is made by the series connection of up to several hundred elementary cells. Each individual cell shares a common metallic plate (so-called bipolar plates) with the neighboring cells.

2.2.3 Performances

As discussed in Section 2.1, the cell efficiency is a function of the operating current density. Higher operating current densities are required to reduce capital expenses but at the same time, lower current densities are required to reduce operational costs (in particular, the electricity consumption per mass unit). A compromise has to be found. The typical polarization curve of an alkaline water electrolysis cell is plotted in Fig. 2.6. Usually, operating current densities are limited to the 400–500 mA/cm^2 range and volumetric stack densities to ca. 15–20 L/Nm^3 H_2 are achieved. The different contributions to the total electrolysis voltage are also plotted in Fig. 2.6. The ohmic drop across the electrolyte and the oxygen (OER) and hydrogen (HER) evolution reaction overvoltages equally contribute to power losses.

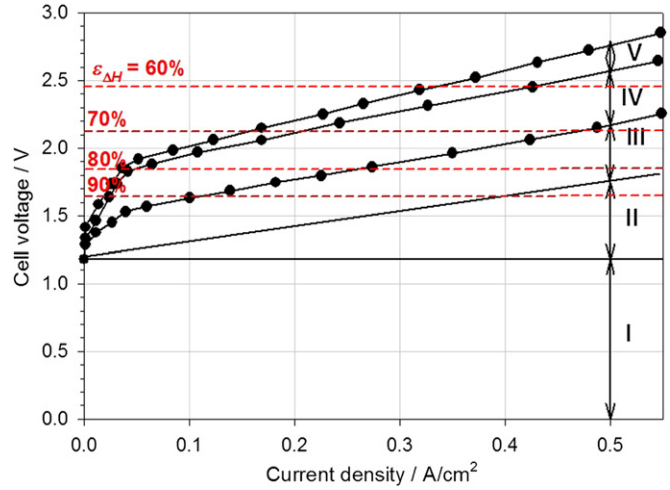

FIGURE 2.6 Electrochemical performances of a conventional alkaline water electrolysis cell. I, thermodynamic voltage; II, ohmic drop in the electrolyte; III, anodic overvoltage associated with the OER; IV, cathodic overvoltage associated with the HER; V, ohmic drop in the main power line. $\varepsilon_{\Delta H}$ = enthalpy efficiency. (For color version of this figure, the reader is referred to the online version of this book.)

The specific energy consumption to produce hydrogen ranges from 4.1 to 4.5 kWh/Nm^3 H_2 at 0.45 A/cm^2.

2.2.4 Technology Developments and Applications

Alkaline water electrolysis is known as the main process for the water-splitting reaction. Military applications related to the use of hydrogen isotopes boosted the development of the technology. The first plants for the electrolysis of heavy water and the production of deuterium were built in Norway. Nowadays, several companies are manufacturing alkaline electrolyzers for the production of hydrogen of electrolytic grade: NEL Hydrogen (a former department of Norsk Hydro Co., Norway)[8]; Hydrogenics Corporation[9] (which acquired Stuart Energy Systems Corp. in 2005); Teledyne[10] (Teledyne Energy Systems, Inc. is a subsidiary of Teledyne Technologies Inc, Maryland, USA); the Russian company "Uralkhimmash"[11]; De Nora (Italy), whose main products are electrolytic cells for chlorine production. The production capacity of industrial systems is usually in the 5–500 Nm^3 H_2/h.

Uralkhimmash produces a range of alkaline electrolyzers (Fig. 2.7). Main characteristics are compiled in Table 2.3. The electrodes of all electrolyzers are made of profiled steel coated with nickel. Diaphragms are still made of asbestos. The table shows that the specific weight and size characteristics of electrolyzers are very high and do not vary greatly with productivity growth. Thus, the electrolyzer mass of FV-250M is about 60 tons, and the

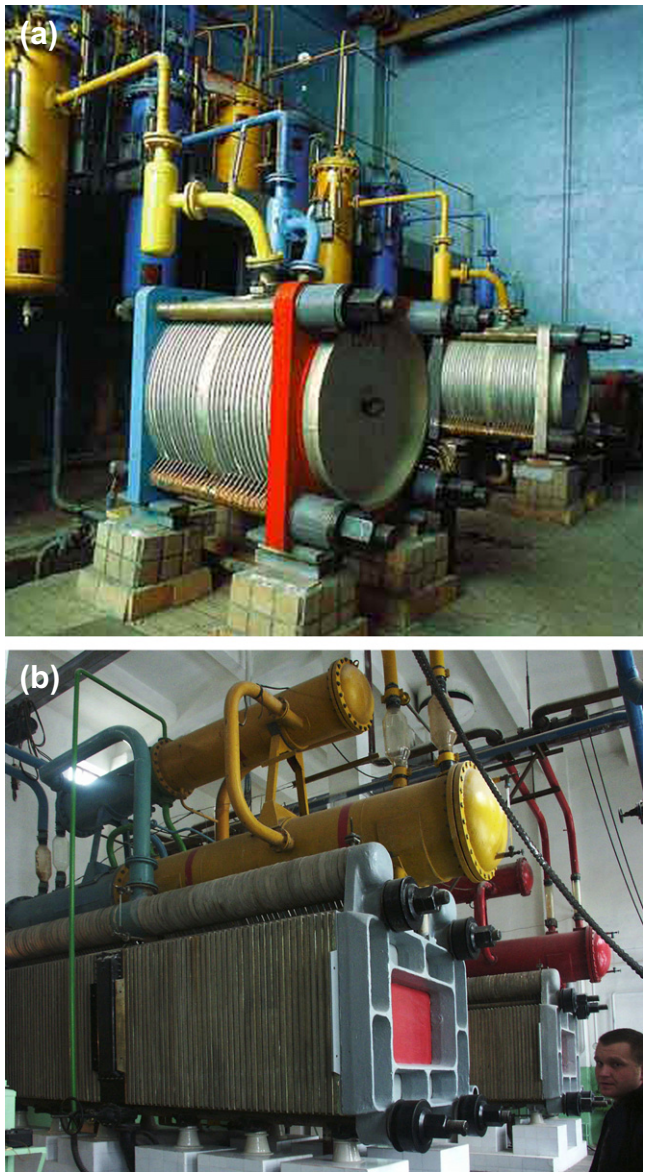

FIGURE 2.7 Electrolysis modules by JSC "Uralkhimmash" (a) SEU-40 and FV-500 (b). (Figures included in electrolyzers' names indicate hydrogen delivery rate in Nm^3/h.) (For color version of this figure, the reader is referred to the online version of this book.)

size is $7.95 \times 3.64 \times 6.54\,m^3$. The size and weight of analogs from other companies are usually 20–30% less.

NEL Hydrogen (Norway) is a world producer of electrolytic systems (Fig. 2.8). Electrolyzers operating at atmospheric pressure can deliver 50–485 Nm^3/h. Energy consumption is usually 4.1–4.3 $kWh/H_2\,Nm^3$ at current densities up to 0.3 A/cm^2. Line current is up to 5150 A. Hydrogen purity is 99.9%, operating temperature is 80 °C, and the electrolyte is a 25% solution of KOH. The area of $4 \times 13.5\,m^2$ is needed to install the electrolyzer that produced 485 Nm^3/h. Pressurized electrolyzers operating at 1.2 MPa and delivering up to 65 Nm^3/h are also commercially available.

The Canadian company Stuart Energy Systems Corp. (now Hydrogenics)[9] produced bipolar and monopolar systems. Monopolar electrolyzers are easy to design and require low maintenance, but they are much heavier and larger and this reduces the application field. Technical characteristics of monopolar cell type EI-250 manufactured over many years by Electrolyzer Company (subdivision of Stuart Energy Systems Corp.) are compiled in Table 2.4.

The applications of water electrolyzers by the Electrolyzer Company are in ammonia synthesis, hydrogen peroxide synthesis, oxygen production and hydrogen isotope separation. The company manufactures self-contained electrolysis systems for meteorological stations. Electrolyzer Company developed one of the first pilot stations for filling 200 buses per day, fueled by hydrogen compressed up to 400 bar.

In 2005, Stuart Energy Systems Inc. (Canada) and Vandenborre Hydrogen Systems (Belgium) formed Hydrogenics Corporation that manufactures electrolysis systems with hydrogen productivity up to 120 Nm^3/h (Fig. 2.9). Operating pressure is up to 25 bar, hydrogen purity is 99.9% and oxygen purity is 99.5%. Specific energy consumption is 4.8–4.9 $kWh/m^3\ H_2$, taking into account the energy required for the operation of supporting systems. The Teledyne Company produces electrolyzers that can deliver up to 150 m^3/h (Fig. 2.10). The water electrolysis stack is positioned at the bottom of the case. Two cylindrical liquid–gas separators (water–H_2 and water–O_2) are installed above. Ancillary equipment includes water circulation, water purity, electricity and heat management sensors for remote monitoring. The compression system and hydrogen storage units are included.

Alkaline water electrolyzers are manufactured for a wide range of market applications. Industrial hydrogen markets are growing fast. Major industrial gas-consuming industries are (1) electric power generator cooling in power plants (it is estimated that over 16,000 hydrogen-cooled generators are installed worldwide) and the addressable market is estimated at $2000 million with payback typically less than 1 year; (2) semiconductor manufacturing; (3) flat panel computers and TV screen producing units; (4) heat treatment plants and (5) analytical chemistry laboratories. Laboratory markets are also significant: (1) laboratory gas generators represent an estimated $60.0 million market worldwide and (2) hydrogen can potentially be used in place of helium as gas carrier in gas analyzers (or as fuel gas for flame detectors). Other industrial markets are glass manufacturing; food processing; meteorology; heat treating and welding industry. Hydrogen as an energy carrier is opening the way to new applications such as management of smart grids for more energy flexibility; chemical storage of renewable energy

TABLE 2.3 Technical Characteristics of Electrolyzers SEU and FV

	Electrolyzer				
Parameters	**SEU-4M-10**	**SEU-3M-10**	**SEU-20**	**SEU-40**	**FV-250M**
Operating pressure, MPa	1	1	1	1	0.1
Operating temperature, °C	80	85	85	90	85
Voltage, V	72	78	100	200	180.4
Gas purity, %					
Hydrogen	99.0	99.0	99.7	99.7	99.5
Oxygen	98.0	98.0	99.5	99.5	98.5
Volumetric efficiency, m^3/h					
Hydrogen	4	8 (max 12)	20.5	41	260
Oxygen	2	4 (max 6)	10.25	20.5	130
Size characteristics, mm					
Length	1700	2050	2400	4100	7950
Width	610	915	1060	1060	3640
Height	830	1080	1780	1785	6540
Weight, kg	1290	3032	4720	7435	59,420
Time to failure, h	11,500	11,500	11,500	11,500	11,500
Established resource to overhaul, h	25,500	25,500	25,500	25,500	25,500
Service life, years	10	10	10	10	10

sources and hydrogen refueling stations for automotive applications.

2.2.5 Limitations, Recent Advances and Perspectives

Alkaline water electrolysis is a mature technology. Several megawatt industrial electrolyzers are used in the industry for the large-scale production of hydrogen in view of different end-uses. The industry has developed electrolyzers that can deliver up to approximately 60 kg/h ($\approx$670 Nm^3/h). From an economic viewpoint, the lifetime of these systems (several tens of thousands of hours of operation) can be considered as satisfactory for continuous operation and is profitable. However, current alkaline electrolysis cells can hardly operate at very low current density, a limit in view of emerging markets of great potential. In particular, this is a limit in terms of flexibility in load-following operation, which will be required for operation with renewable energy sources. From the material viewpoint, major research efforts concern the development of advanced diaphragms with adapted electrodes/catalysts. Most efficient diaphragms used to be made of asbestos that is now forbidden in most countries. The replacement of asbestos by composite ceramic/polymer materials is proposed but there is still room for improvement.[12] Enhanced electrocatalysis is also an issue. Attempts have been made to identify alternative electrocatalysts, and the electrocatalytic properties of some transition metal macrocycles have received attention.[13] From the performance viewpoint, higher efficiencies can be obtained using advanced alkaline water electrolyzers. Prototypes delivering up to 25 Nm^3 H_2/h have been developed over the last decades.

FIGURE 2.8 Alkaline water electrolysis modules developed by NEL Hydrogen. (For color version of this figure, the reader is referred to the online version of this book.)

TABLE 2.4 EI-250 Type Cell Characteristics

Parameters	Value
Productivity of hydrogen, m^3/h	42
Electrolysis temperature, °C	70
Nominal current density, kA/m^2	2.5
Nominal voltage, V	1.85
Energy efficiency, %	81
Energy consumption, kW/m^3 H_2	4.4
Overall dimensions of the electrolyzer, m	$1.1 \times 1.8 \times 2.1$
Weight of the electrolyzer, tons	6.6

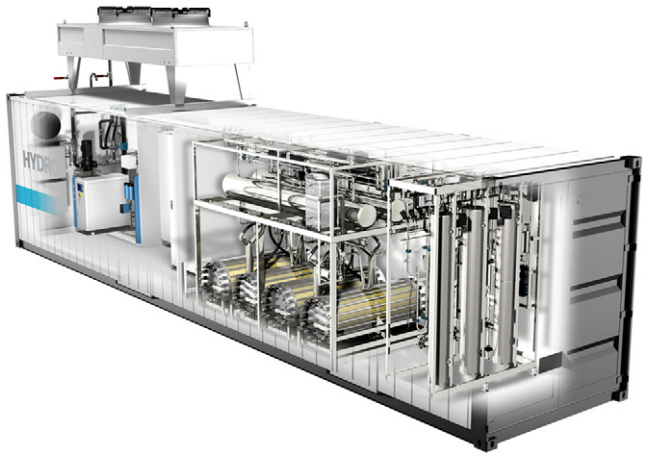

FIGURE 2.9 Alkaline hydrogen generator HySTAT by Hydrogenics Corporation. Productivity is 24 kg of hydrogen per day. (For color version of this figure, the reader is referred to the online version of this book.)

Such units using the zero-gap configuration are reported to operate at higher current densities $1.25\,A/cm^2$, 120 °C, 5–40 bars. The electrical power consumption (at $200\,mA/cm^2$) is $3.81\,kWh/Nm^3$ H_2 at 90 °C (≈78% efficiency) and $3.65\,kWh/Nm^3$ H_2 at 120 °C (≈80% efficiency) (stainless steel).

FIGURE 2.10 "Titan" electrolyzer by Teledyne Company. (For color version of this figure, the reader is referred to the online version of this book.)

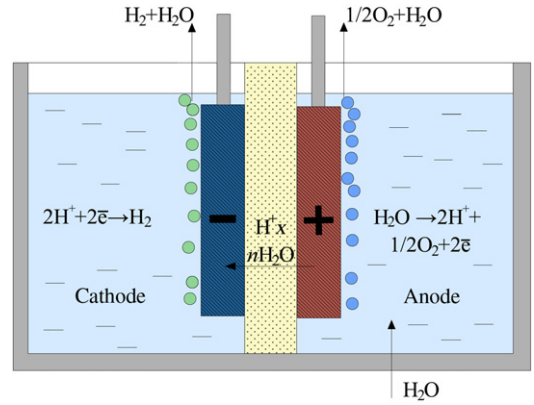

FIGURE 2.11 Schematic diagram of PEM electrolysis cell. (For color version of this figure, the reader is referred to the online version of this book.)

2.3 PROTON-EXCHANGE MEMBRANE WATER ELECTROLYSIS

2.3.1 Principles

The general features of proton-exchange membrane (PEM) water electrolysis cells are pictured in Fig. 2.11. Two electrodes are pressed against a proton-conducting polymer electrolyte thus forming a so-called membrane electrode assembly (MEA). The MEA is immersed in pure (18 MΩ cm) water. Mobile protons species remain confined inside the polymer membrane.

Oxygen evolution tales place at the anode:

$$H_2O \rightarrow \frac{1}{2}O_2 + 2e^- + 2H^+ \quad (E^0 = 1.229\ V \text{ at } 25^\circ C) \tag{2.26}$$

The hydrogen ions are transported across the ion-exchange membrane (SPE) and hydrogen is generated at the cathode:

$$H^+ + 2e^- \rightarrow H_2 \quad (E^0 = 0\ V \text{ at } 25^\circ C) \tag{2.27}$$

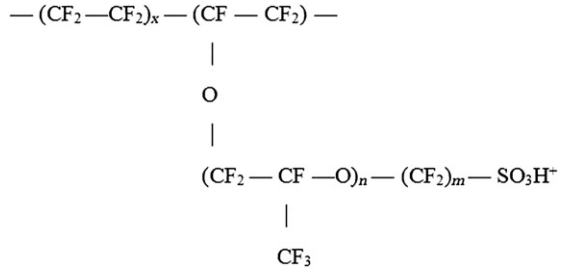

FIGURE 2.12 The structural formula of Nafion® membrane by DuPont de Nemours.

The overall reaction is:

$$H_2O \rightarrow H_2 + \frac{1}{2}O_2 \quad (E^0 = 1.229\ \text{V at } 25^\circ\text{C}) \qquad (2.28)$$

From a historical perspective, the development of PEM water electrolyzers started in the 1960s at General Electric Co. (USA) when appropriate proton-conducting polymers became commercially available.[14] The most famous one is Nafion® developed by DuPont de Nemours Co.[15] This is a perfluorinated polymer with functional sulfonic acid end-groups (Fig. 2.12).

Although protons remain inside the membrane, the acidy is very high (similar to that of a 1M sulfuric acid solution). Therefore, only noble metal catalysts that can sustain such acidity are required at both the anode and cathode. PEM water electrolysis is an expensive technology and the first electrolyzers for space vehicles and oxygen generation in submersibles were developed.

2.3.2 Cell Components

SPE water electrolyzers, also called PEM electrolyzers in modern literature, are considered the safest and most effective technology to produce hydrogen from water.[16] A key component of SPE systems is the ion-exchange membrane. In 1959, W. Grubb was the first to propose the use of organic cation-exchange membrane as solid electrolyte in electrochemical cells, in particular, for fuel cells in view of the US space program. First attempts were made using sulfonated polystyrene. However, its chemical stability was not sufficient for practical applications and the performances of fuel cells using this kind of membrane were significantly lower than those obtained with water–alkaline fuel cells.[17,18]

Today, new SPE materials made of perfluorinated phosphonic acid copolymers have appropriate properties (relatively low resistance, high mechanical strength and good chemical stability) for operation in fuel cells and water electrolyzers. As already mentioned, the most famous brand of this kind of membranes is Nafion® by DuPont de Nemours Co. (USA).[19] Ion-exchange perfluorinated membranes are elastic and transparent films, several tens to several hundreds micrometers thick, with a smooth surface. From the chemical viewpoint, the material is a copolymer of tetrafluoroethylene containing grafted sulfonic functional groups. The material has a high chemical stability, in particular, in the presence of native oxygen at high potential values, thus offering a resource for several tens of thousand hours of operation. However, even today, the problem of chemical stability of these materials is not completely solved. In particular during fuel cell operation, it has been shown that the incomplete (two electrons) reduction of oxygen can lead to the formation of hydrogen peroxide which, although formed in small amounts, can lead to a gradual degradation of the membrane.[20] The consequence is an increasing gas permeability during operation and a decrease in cell efficiency (the cell voltage and fuel efficiency tend to decrease with time). Hydrogen peroxide can also be formed during water electrolysis.

In contact with water, membrane swelling and dissociation of the ion-exchange groups occurs. As a result, protons can move freely in the volume of the polymer from one electrode to another through a system of fixed sulfonic acid groups. The acidity of these materials is equivalent to that of 10% sulfuric acid aqueous solutions. The resistivity of the membrane is significantly larger than the resistance of aqueous solutions of alkalis (11–12 Ohm cm at 20 °C and 5–6 Ohm cm at 80–90 °C). It is therefore necessary to use thin (100–300 μm thick) membranes to reduce ohmic losses during electrolysis but the use of smaller thicknesses is not appropriate because the permeability of gases through the membrane becomes too important.

There is no liquid electrolyte, so the electrodes should be held tightly to the membrane (the so-called zero-gap configuration), and to provide high surface contact between the catalyst (electronic conductor) and the electrolyte, the catalyst is deposited on the surface of the membrane with the ion-exchange electrolyte.[21] The resulting electrocatalytic composition has mixed electronic–ionic conductivity and has the porosity (30%) required for removal of gaseous reaction products. Porous current collectors are pressed firmly against catalytic layers and adjacent electrolysis cells are separated by metallic bipolar plates. It should be noted that zero-gap cells were also used in water–alkaline electrolyzers to reduce ohmic losses, but the increasing rate of mutual products' transport through the membrane, especially at high pressures, is problematic.

Highly dispersed catalysts based on platinum group metals (PGM) are used in PEM water electrolyzers. Ruthenium has the highest catalytic activity in the reaction of oxygen evolution, but Ru is not stable at the anode potentials of 1.23 V in acidic media. Currently,

the most widely used anode catalyst is Ir (or oxide), as well as mixed oxide compositions, such as Ru_xIr_y $Sn_{1-x-y}O_2$ and $Ru_xIr_yTi_{1-x-y}O_2$ with catalyst loadings of ca. 2.0 mg/cm^2. Pt or Pd can be used at the cathode, including the carbon carrier. Pt can also be used as an anode catalyst, but in this case, the cell voltage is 100−200 mV higher. Porous titanium is usually used for the current collectors, the thickness is 600−1000 μm, porosity is >30%. The current collector is used to apply the required potential to the catalyst, supply reagent to the interfaces and remove reaction products. It should be noted that PGMs are also used to protect current collectors against surface oxidation (e.g. Pt coatings of ≈1 mg/cm^2).

The main advantages of PEM water electrolysis are as follows:

1. possibility of operating the cells at high (several A/cm^2) current density;
2. High efficiencies can be obtained, even at high current densities; this is because a PEM cell is a thin zero-gap cell and thus, ohmic losses are minimized and the overall efficiency is improved due to a lack of screening of the electrodes by gas bubbles; also, highly dispersed catalyst particles are used; they offer a large specific surface area and overvoltages are significantly low;
3. De-ionized water is used as sole reactant; as a result, high-purity gases are produced;
4. High dynamic range (0−100% production range reached within less than 50 ms).

The main drawbacks of PEM water electrolysis are as follows:

1. Capital expenses of not only MEA materials (catalysts and SPE) but also of other cell components (titanium is commonly used) are still too high;
2. Need for high-purity water and therefore expensive purification units;
3. Large-scale systems (>100 Nm^3/h H^2) still need to be developed.

2.3.3 Performances

Typical polarization curves measured on PEM water electrolysis stacks are plotted in Fig. 2.13. State-of-the-art range of operation of commercial PEM water electrolyzers is delineated by the gray rectangle. An enthalpy efficiency of 80% is commonly achieved at 1.0−1.5 A/cm^2 using platinum for the HER at the cathode and iridium oxide at the anode for the OER. As can be seen from Fig. 2.13, the membrane thickness provides a significant contribution to the cell efficiency. These electrolyzers deliver high-purity hydrogen (≥99.99% after drying), oxygen from the anode being the main impurity. Operation

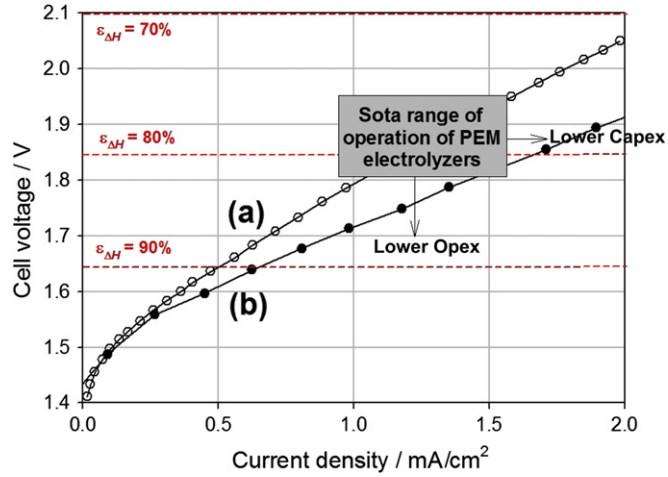

FIGURE 2.13 Current−voltage polarization curves of conventional PEM water electrolysis cells at 80 °C using platinum for the HER and iridium oxide for the OER. $P = 1$ bar: (a) membrane thickness = 200 μm; (b) membrane thickness = 150 μm. (For color version of this figure, the reader is referred to the online version of this book.)

lifetime of 10,000 h and longer is a common good practice. Reduced maintenance operations are required when high-purity water is fed to the electrolyzer. The energy consumption is usually low (≈3.9 kWh/m^3 at 1 A/cm^2) and the technology offers the possibility of delivering hydrogen at high pressure (up to 3 MPa and more) directly in the cell[21,22] in order to favor the direct storage of compressed hydrogen and reduce gas-drying costs. R&D programs are aimed at decreasing both operational and capital expenses. Reduction of cell voltage at constant current density is an important goal. This can be achieved by using more efficient electrocatalysts and can reduce the system Opex (operational expenses). Higher operating current densities at constant cell voltage is another important goal. This can be achieved by using thinner membranes and can reduce the system Capex (capital expenses).

2.3.4 Technology Developments and Applications

Currently, the major manufacturers of industrial water PEM electrolyzers are Hamilton Sundstrand (USA),[23] Proton OnSite (USA)[24] and Yara (Norway).[25] These companies have created electrolyzers operating under pressures up to 2.8 MPa with capacity up to 26 m^3/h, and it is possible to combine electrolysis installations with capacity of 260 m^3/h (Figs 2.14 and 2.15).

The German company H-tec[26] produces small demonstration samples of water PEM electrolyzers for educational purposes. Researches and developments of PEM electrolyzers are conducted in many countries, for example, in France, Japan, and India.[27,28] The

FIGURE 2.14 PEM electrolyzer HOGEN S Series by Proton OnSite. Productivity, $1\,m^3H_2/h$; electric power consumption, 5.6–9.0 kWh/m^3; electrolysis voltage, 2.3–3.8 V; output pressure, 1.4 MPa; size, $97 \times 78 \times 10^6\,cm^3$; weight, 215 kg. (For color version of this figure, the reader is referred to the online version of this book.)

FIGURE 2.15 PEM electrolyzer by Yara (Norsk Hydro Electrolysers). Productivity, $10\,Nm^3$ H_2/h; electric power consumption, 4.4 kWh/m^3; output pressure, 3.0 MPa; hydrogen purity, 99.9% (O_2 as main impurity). (For color version of this figure, the reader is referred to the online version of this book.)

possibility of significant progress in this area has been demonstrated through the Japanese WE-NET program, where a cell was developed and successfully tested with surface area of 2500 cm^2, operating voltage of 1.556 V at 80 °C, current density of 1 A/cm^2 and an energy conversion efficiency of 95.1%. This efficiency is explained by the proximity of the electrolysis voltage to the thermoneutral voltage (ca. 1.48 V). Development of advanced PEM electrolyzers with elevated pressure (up to 5.0 MPa) has been successfully implemented in the project GenHyPEM of 6th Framework European Program.[29] The objectives of this project were development of new gas-tight membranes, high-performance nanocatalysts (including nonplatinum) and biporous current collectors to improve the efficiency of mass transfer processes. In Russia, researches and developments of water PEM electrolysis systems for more than 20 years are conducted in the National Research Center "Kurchatov Institute", Federal State Unitary Enterprise "Red Star" and other organizations. Currently, PEM electrolyzers have been created with capacity from a few milliliters to several cubic meters of hydrogen per hour (Fig. 2.16) for various purposes.[30]

Potentially, market applications of PEM water electrolyzers are similar to those of their alkaline counterparts although commercially available systems have lower production capacities than the alkaline systems.

2.3.5 Limitations, Recent Advances and Perspectives

As indicated in the previous section, an increasing number of private companies are active in the field and PEM technology offers a number of advantages. A brief comparison of PEM and alkaline water electrolysis technologies is provided in Table 2.5.

The main difference between the two technologies is that the alkaline process is well established, with impressive track records in terms of market assessment. Capital expenses are more favorable, even though alkaline electrolyzers operate at much lower current densities (at least two times lower), and thus, operational costs (in particular energy costs) are also more favorable. Moreover, the technical know-how gained over almost a century of operation in the development of large-scale systems also speaks in favor of alkaline systems. However, PEM electrolysis offers more significant perspectives in terms of improvement. It can be

FIGURE 2.16 PEM electrolysis stacks developed by NRC "Kurchatov Institute". (a) Stack with productivity of 25 l/h, (b) Stack with productivity of 125 l/h and operating pressure of 30 bar, (c) Stack with productivity of 1.5 m^3 and operating pressure of 30 bar, (d) Electrolysis module with bi-stack configuration with productivity of 2.5 m^3 and operating pressure of 130 bar. (For color version of this figure, the reader is referred to the online version of this book.)

TABLE 2.5 Comparison of Alkaline and PEM Water Electrolysis Technologies

	Alkaline electrolysis	**PEM electrolysis**
Electrolyte	Caustic solution	Polymer electrolyte
Nominal current density	0.45 A/cm^2	1.0 A/cm^2
Energy consumption	4.35 kWh/Nm^3 at 0.45 A/cm^2	4.35 kWh/Nm^3 at 1.0 A/cm^2
Maximum current density	0.8 A/cm^2	10 A/cm^2
H_2 delivery pressure	Up to 30 bar	Up to 700 bar
H_2 purity (dry basis)	≥99.9%	≥99.99%
Lifetime	≥60,000 h	≥25,000 h
Dynamic range	0–100%	0–100%
Volumetric stack density	16 L per Nm^3/h H_2	0.5 L per Nm^3/h H_2

said that in terms of market applications, PEM electrolyzers will probably become a serious competitor of the alkaline technology in the coming years, even for the large-scale production of hydrogen. To reach this goal, cost is of course the main issue and substantial progresses are needed to reduce capital expenses (a simplified cost analysis is provided in Fig. 2.17). MEA cost (approximately two thirds for the SPE and one third for the PGM catalysts including platting process) accounts for only 12% of the entire system cost. Cost of bipolar plates and flow fields is two times larger than MEA cost.

Some significant advances have been made during the last years and there is still room for further improvements. They are the subjects of many international R&D programs, in the public sector and in the industry.

2.3.5.1 *Reduced PGM Contents*

A first option to bring cost down was to reduce PGM contents. This can be achieved by dispersing

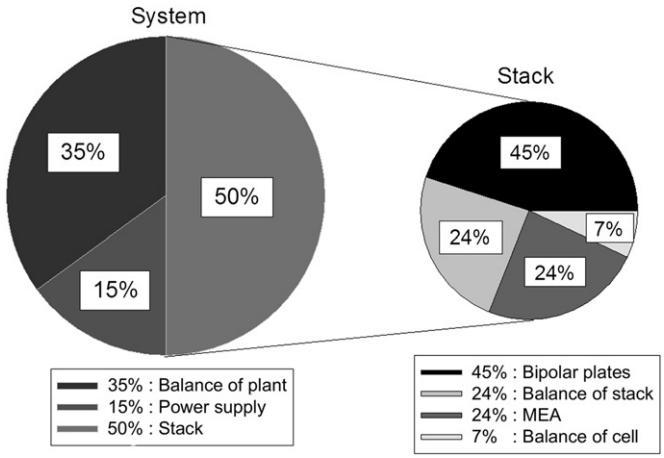

FIGURE 2.17 Cost analysis of PEM water electrolyzers.

nanoparticles at the surface of electronic carriers of large surface area. Similar to PEM fuel cell technology, carbon-supported platinum nanoparticles are commonly used now at the cathode of PEM electrolyzers for the HER. At the anode, mixed oxides (e.g. RuO_2–IrO_2–SnO_2) are increasingly used for the OER. PGM loadings have been significantly reduced. Pt loadings at cathodes are now in the 0.3–0.5 mg/cm^2 range (Fig. 2.18). Palladium (which is significantly less expensive than platinum and even more active) can also be used for that purpose. Like platinum, palladium can be deposited at the surface of carbon carriers.[21]

2.3.5.2 Non-PGM Catalysts

Another option to reduce MEA costs is to develop non-PGM electrocatalysts. Some advances have been made in this field over the last years.[31] Some typical polarization curves measured on a PEM water electrolyzer operating at 80 °C are plotted in Fig.2.19. The overall efficiency differs significantly from one curve to the other, highlighting the role of electrocatalysts. A first reference curve (Pt/Pt) is obtained using pure platinum particles for both the OER and the HER. As can be seen from Fig. 2.19, an enthalpy efficiency of ≈65% is obtained at 1 A/cm^2. More efficient results are obtained when pure iridium particles are used at the anode for the OER (Pt/Ir): an efficiency of ≈82% is obtained at 1 A/cm^2. Because of the increasing cost of noble metals, there is a need to find cheaper materials. Over the last years, several non-PGM catalysts have been identified and used at the cathode of PEM water electrolysis cells in place of platinum. For example, polyoxometalates can be used for that purpose. In Fig. 2.19, three additional curves (red circles, curves labeled 1, 2, 3) were obtained with increasing loadings of α-$H_4SiW_{12}O_{40}$ for the HER and iridium metal for the OER. Although the electrochemical performances are not as good as those obtained with the Pt/Ir reference curve, results are encouraging: an enthalpy efficiency close to 70% has been obtained at 1 A/cm^2. Another example is provided by cobalt-based clathrochelates.[32] These results offer new and interesting perspectives for application in the industry.

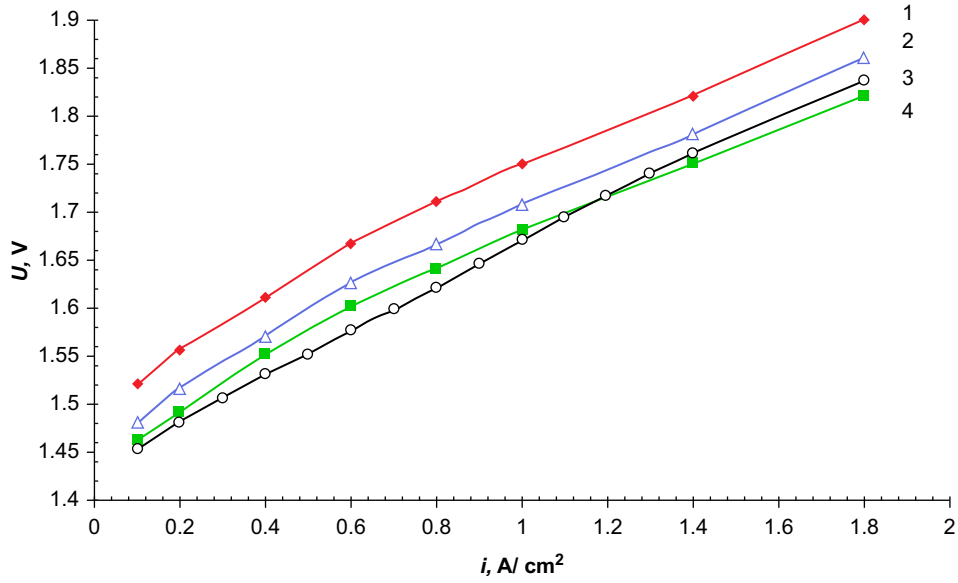

FIGURE 2.18 Current–voltage polarization curves measured at 90 °C on PEM water electrolysis cells with different catalysts. 1, cathode: Pt30/C—2.0 mg/cm^2; anode: Ir—2.4 mg/cm^2; 2, cathode: Pt30/C—2.0 mg/cm^2, anode: RuO_2(30%)–IrO_2(32%)–SnO_2(38%)—2.0 mg/cm^2; 3, cathode: Pd40/C—2.4 mg/cm^2, anode: Ir—2.4 mg/cm^2; 4, cathode: Pt30/C—2.0 mg/cm^2, anode: RuO_2(50%)–IrO_2(50%)—2.0 mg/cm^2 (Pt30/C is 30 wt% Pt on carbon carrier). (For color version of this figure, the reader is referred to the online version of this book.)

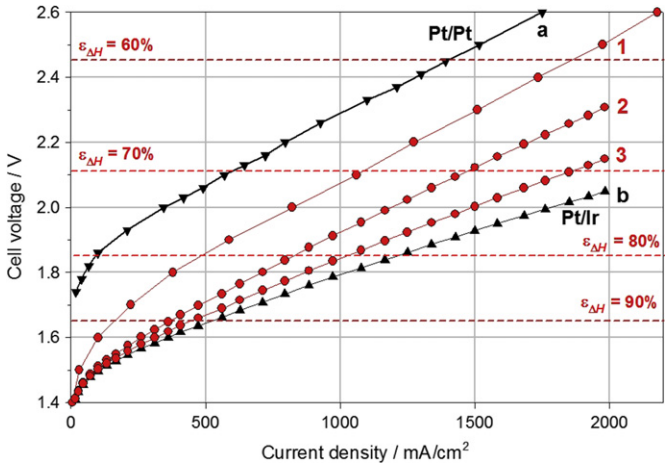

FIGURE 2.19 Current-voltage characteristics of PEM water electrolysis cells (7 cm^2) at 90 °C; (a) reference curve with Pt for both HER and OER; (b) reference curve with Pt for the HER and Ir for the OER; (•) Ir for the OER (2.5 mg/cm^2) and a-$H_4SiW_{12}O_{40}$ (at different concentrations) for the HER: (1): 0.2 mg/cm^2; (2): 0.5 mg/cm^2; (3): 0.8 mg/cm^2. (For color version of this figure, the reader is referred to the online version of this book.)

Such approaches, however, require additional R&D efforts. They could also have some positive side effects since the replacement of platinum would release the constraints on feed-water resistivity (Pt is highly sensitive to metal underpotential deposition).

2.3.5.3 Higher Operating Current Densities

To further reduce expenses, it is also necessary to develop new materials in order to increase current density (lower capital expenses) and to increase operating temperature (lower operational costs). These fields of material science are of growing interest, also driven by potential applications in the PEM fuel cell industry. Whereas in PEM fuel cells, maximum operating current densities come from mass transfer limitations (transport of gaseous reactant to the reactive centers), there is no such limitations in water electrolysis cells. Significantly high current densities (10 A/cm^2) have been demonstrated. The main problem comes from the insufficient conductivity of the electrolyte and inappropriate ohmic losses. Better efficiencies can be obtained by using thinner membranes but in turn, gas cross-permeation effects tend to reduce faradic efficiency and reduce gas purity.

2.3.5.4 Higher Operating Temperature

Concerning the SPE, there is a need to develop polymer proton conductors for operation at more elevated temperatures. Research in this field is driven by potential applications in the H_2/O_2 fuel cell industry for automotive applications. Significant progresses have been made in the development of improved perfluorinated polymer materials operating in the 120–150 °C temperature range (e.g. using materials such as Aquivon® products from Solvay Solexis Co.). Some of these materials have been successfully tested in PEM water electrolysis cells. Also, polybenzimidazole materials operating at temperatures ca. 200 °C have been developed. They may offer in the future some interesting possibilities to operate water electrolysis cells in this very interesting temperature range.

2.3.5.5 Higher Pressure Operation

PEM water electrolysis technology offers the possibility to increase operating pressure for the direct storage of hydrogen in pressurized vessels. This is a very attractive prospect for stationary systems with relatively small (up to 100 kW) power capacity. This is a challenging field of research. The main problem is to reduce the rate of gas cross-permeation by diffusion through the membrane which, in turn, can reduce the current efficiency and lead to the formation of hazardous H_2/O_2 explosive gas mixtures. Over the last years, several experiments have been reported in the literature. A PEM electrolyzer that can deliver 10 Nm^3/h H_2 at a pressure up to 13.0 MPa has been developed and tested at the Kurchatov Institute within the frame of a Federal R&D project. Typical polarization curves measured at different operating temperatures and pressures are plotted in Fig. 2.20.

It can be seen that temperature is the parameter that has the most significant effect on the process efficiency. Pressure has a less pronounced effect. From a thermodynamic viewpoint, an increase of pressure tends to increase the electrolysis voltage. But at high current densities, this effect is balanced by a better kinetics (transport of gas bubbles away from the interfaces) and as a result, higher operating pressures do not negatively impact cell performances. Increased operating pressure is also necessary to perform water electrolysis at temperatures above 100 °C.

At this stage, it is worth mentioning the development of so-called reversible systems or unitized regenerative fuel cells, i.e. electrochemical devices that can operate either like a fuel cell or an electrolyzer (a kind of H_2/O_2 battery).[33] Reversible PEM systems are interesting to create a stand-alone (decentralized) energy system based on intermittent power sources, such as renewable energy sources.

2.3.5.6 Other Cell Components

As shown in Fig. 2.17, the MEA is not the sole component responsible for the expensive capital costs in PEM water electrolyzers. Other cell components also add significant contributions. Bipolar plates, flow fields and current distributors are two times

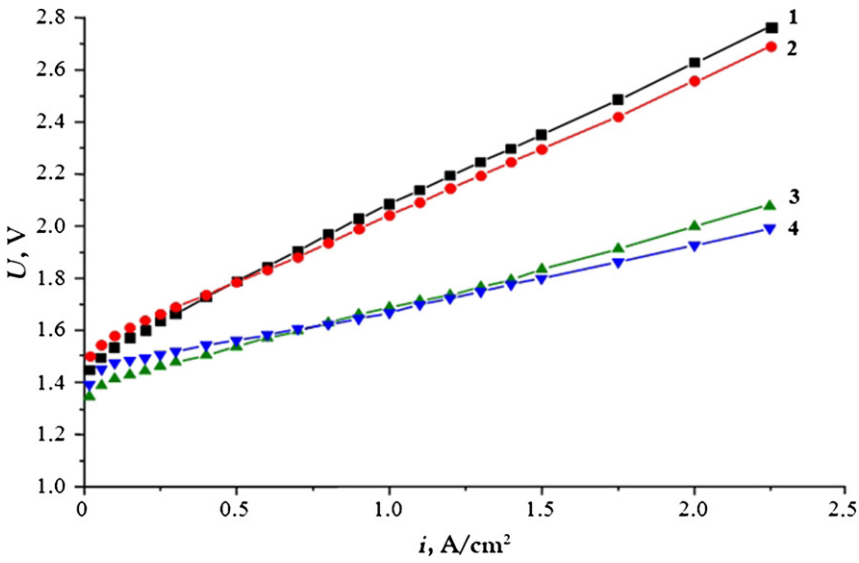

FIGURE 2.20 The current–voltage characteristics of PEM electrolysis cell at different operating temperatures and pressures. 1, $T = 30\,^{\circ}C$, $P = 1$ bar; 2, $T = 30\,^{\circ}C$, $P = 25$ bar, 3, $T = 90\,^{\circ}C$, $P = 1$ bar, 4, $T = 90\,^{\circ}C$, $P = 25$ bar. (For color version of this figure, the reader is referred to the online version of this book.)

more expensive. This includes raw material costs and surface treatment (titanium bipolar plates and current collectors) to reduce contact resistance (Pt coatings are expensive, nitrides, carbides, etc.). Main challenges for PEM water electrolysis are to identify and synthesize alternative materials with performances similar to those used in state-of-the-art technology.

2.3.5.7 *Extended Lifetime of Operation*

In the industry, PEM electrolyzers have demonstrated their ability to operate during several tens of thousand hours. Extending the lifetime of operation offers the possibility to further bring capital expenses down. Lifetime operation in the upper 10,000–100,000 h time range is the target. PEM water electrolysis is well suited for dynamic operation. Several studies have shown that performances remain stable and that the electrolyzers can provide rapid response time to current signals. Therefore, high dynamic ranges (0–100% production range reached within less than 50 ms) are accessible. This is of particular interest when transient renewable energy sources are used as power sources. PEM water electrolyzers can add flexibility to the management of smart grids.

2.4 HIGH-TEMPERATURE WATER ELECTROLYSIS

2.4.1 Principles

The general features of SOWE cells are pictured in Fig. 2.21. Oxide-ion conducting ceramics is used as solid electrolyte and cell separator. Water molecules are reduced at the cathode according to:

$$H_2O_{(g)} + 2e^- \rightarrow H_{2(g)} + O^{2-} \qquad (2.29)$$

The resulting oxygen ions O^{2-} migrate to the anode, where oxygen evolves according to:

$$2O^{2-} - 2e^- \rightarrow O_2 \qquad (2.30)$$

Such solid-oxide electrolysis cells usually operate in the 800–1000 °C temperature range. The most common electrolyte (like in solid-oxide fuel cell (SOFC) technology) is zirconia ZrO_2 stabilized with yttrium and scandium oxides.[34–37]

The transport of oxide ions across zirconia is a diffusion process throughout the defects of the crystal structure. The resistivity of the solid electrolyte is larger than the resistance of alkaline solutions and ion-exchange

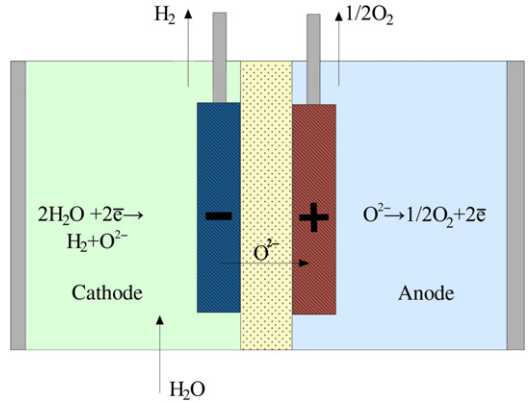

FIGURE 2.21 Schematic diagram of solid-oxide electrolysis cell. (For color version of this figure, the reader is referred to the online version of this book.)

TABLE 2.6 Ionic Conductivity of Several Solid Electrolytes at Different Temperatures

Electrolyte	Conductivity, Ohm/cm		
	880 °C	650 °C	500 °C
$(Bi_2O_3)_{0.8}(SrO)_{0.2}$	2.7×10^{-1}	5.0×10^{-2}	6.0×10^{-3}
$(Bi_2O_3)_{0.8}(BaO)_{0.2}$	–	7.0×10^{-1}	1.1×10^{-2}
$(Bi_2O_3)_{0.75}(Y_2O_3)_{0.25}$	3.5×10^{-1}	1.1×10^{-1}	1.3×10^{-2}
$(Bi_2O_3)_{0.65}(Gd_2O_3)_{0.35}$	2.6×10^{-1}	5.6×10^{-2}	3.5×10^{-3}
$(Bi_2O_3)_{0.85}(Nb_2O_5)_{0.15}$	5.0×10^{-1}	1.1×10^{-1}	1.1×10^{-2}
$(Bi_2O_3)_{0.80}(Ta_2O_5)_{0.20}$	7.3×10^{-2}	1.0×10^{-2}	5.0×10^{-3}
$(Bi_2O_3)_{0.78}(MoO_3)_{0.22}$	1.1×10^{-1}	1.7×10^{-2}	2.6×10^{-3}
$(Bi_2O_3)_{0.78}(WO_3)_{0.22}$	1.5×10^{-1}	4.1×10^{-2}	1.0×10^{-3}
$(ZrO_2)_{0.91}(Y_2O_3)_{0.09}$	2.0×10^{-2}	3.8×10^{-3}	4.6×10^{-4}

membranes (≈30 Ohm·cm even at 900–1000 °C, Table 2.6). Therefore, thin ceramic membranes (30–150 μm) are required for the electrolysis process to reduce ohmic losses as much as possible.

2.4.2 Cell Components

In conventional technology, the main SOWE cell components are stainless steel bipolar plates and manganite-coated stabilized zirconia as solid electrolyte (Fig. 2.22).

2.4.3 Performances

The development of SOWE technology in view of applications in the industry started in the early 1970s. Prototypes using tubular cells and delivering up to 1 Nm^3/h H_2 at 1000 °C have been developed and tested at Dornier Systems Co. Similar developments have been made in parallel by Westinghouse. According to the literature, in spite of encouraging lifetimes and high cell efficiencies (operations for 500 h and efficiencies close to 100% have been reported[38]), experiments have been stopped because of prohibitive costs and lack of short-term commercial applications. Since then, because of the world energy crisis, the situation became gradually more favorable and new R&D programs have been launched.[39,40] Possibility of operation at high current densities with efficiencies close to 100% have been confirmed (e.g. a current density of 3.6 A/cm^2 has been reported at 1.48 V and 950 °C[41]). In addition, the overall efficiency of these solid-oxide cells can be further improved by co-electrolyzing water vapor and carbon dioxide to produce syngas ($H_2 + CO$), that is of great industrial interest, for example for the production of synthetic fuels. Some typical polarization curves measured for these systems are plotted in Fig. 2.23. At such operating temperatures, electrochemical processes are fully reversible and the electrochemical cells can operate either as a fuel cell or as an electrolysis cell. The cell resistance (the slope of the polarization curves) decreases significantly when the temperature increases and current densities of several A/cm^2 can be obtained during the co-electrolysis of water vapor and CO_2. The composition of the syngas can be adjusted by monitoring the composition of the water–CO_2 gas mixtures introduced in the electrolyzer.

High-temperature water electrolyzers using solid-oxide electrolyte[42] was successfully developed in the 1980s at the Institute of the High-Temperature Electrochemistry of the Ural Branch of the Russian Academy of Sciences. The heat balance during electrolysis was more specifically analyzed in order to determine the conditions for which the electrolysis cell does not exchange heat with the surrounding. When the electrolysis cell was operated at constant temperature, it was

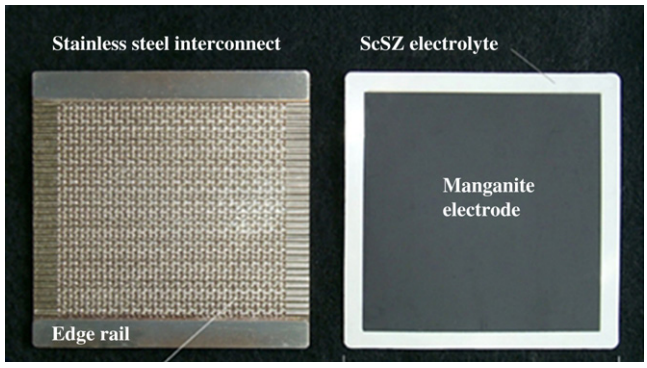

FIGURE 2.22 Photographs of bipolar plates and MEAs used in SOFC technology. (For color version of this figure, the reader is referred to the online version of this book.) *Source: CERAMATEC Co.*

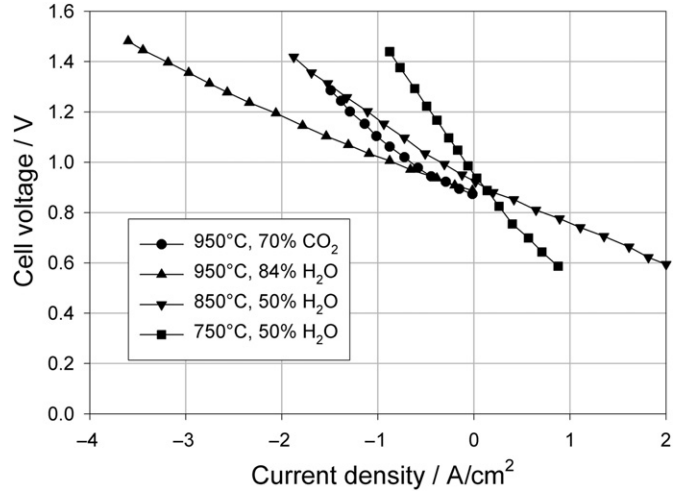

FIGURE 2.23 Polarization curves measured on a 5 × 5 cm^2 SOFC cell.[38]

found that operation at low current density (corresponding to cell voltage less than 1.29 V) without the supply of external heat led to a significant temperature drop inside the stack. The maximum temperature difference between the cell and the environment was found to be ca. 20 °C at a current density of 0.3 A/cm^2. As the operating current density was increased, the temperature difference gradually decreased and at 0.6 A/cm^2 the temperature of the electrolyzer became similar to that of the environment. These results demonstrated that the energy consumption of the water splitting reaction conducted at high temperature requires less electricity compared to low-temperature electrolysis and that the remaining energy requirements can be provided by additional heat supply (for example from high-temperature gas-cooled reactor or solar concentrators).

2.4.4 Technology Developments and Applications

High-temperature water electrolysis cells using ceramic membranes are developed by several companies and research centers: Siemens–Westinghouse (USA–Germany), Institute of the High-Temperature Electrochemistry of Ural Branch of Russian Academy of Sciences (Russia) (Fig. 2.24), National Research Center "Kurchatov Institute" (Russia) and State Scientific Center "AI Leypunsky Physics and Power Engineering Institute" (Russia).

Electrodes are deposited on both surfaces of a thin ceramic membrane used as electrolyte. SOWE cells can have different geometries: planar geometries (similar to cells of other electrolytic cell types), tubular (the electrolyte is in the form of a thin-walled tube), and even more complex configurations such as "honeycomb" shapes (Fig. 2.25). At such elevated temperatures of operation, the need for electrocatalysts is less significant compared to the requirements at lower operating temperatures. It is therefore possible to operate such cells with non-PGM catalysts. The usual material used at the cathode for the HER is a ceramic-metal (cermet) alloy containing Ni and Zr. The usual material used at the anode for the OER is platinum- or strontium-doped lanthanum manganite. However, it is difficult to completely eliminate the use of precious metals; in state-of-the-art technology, they are used to assure appropriate electrical contacts between the cells.

R&D programs were carried out by a group of national laboratories in the USA (supported by the U.S. Department of Energy) in 2006. A demonstration electrolyzer containing 25 planar cells with a hydrogen production capacity of 160 L/h (800 °C) has been developed. The electrolyzer has been tested for 1000 h. During the test, it was found that electrochemical performances tend to decrease significantly, leading to a final loss of

FIGURE 2.24 High-temperature electrolysis for 100 L of hydrogen per hour developed by the Institute of High-Temperature Electrochemistry of Ural Branch of Russian Academy of Sciences. (For color version of this figure, the reader is referred to the online version of this book.)

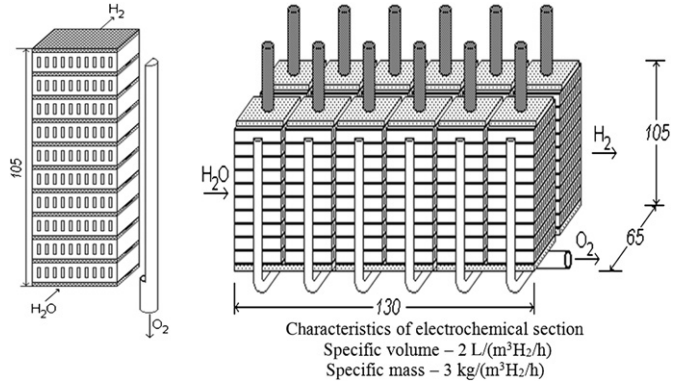

FIGURE 2.25 Schematic diagram of a solid-oxide water electrolyzer developed at the Institute of High-Temperature Electrochemistry of Russian Academy of Sciences.

almost 30%. It was shown that the stability of electrode materials, in particular hydrogen electrode based on nickel and zirconium oxide stabilized with yttrium and scandium (for mixed electronic−ionic conductivity) is not sufficient at high concentrations of water vapor and can lead to the oxidation of the nickel surface. However, work is continuing in this direction and it is planned to build electrolyzers having an input power of 200−1000 kW.

High-temperature solid-oxide electrolysis cells offer the possibility to simultaneously decompose water vapor and carbon dioxide. It can be used to develop effective life support systems, for example, for space and submarine operation. The thermodynamic voltage required at 900−1000 °C in the SOWE cell is less than 1 V and a typical cell voltage of 1.2−1.3 V is commonly used. This corresponds to an electricity consumption of 2.8−3.0 kWh/Nm^3 H_2. However, about 0.4−0.5 kWh/Nm^3 H_2 of heat is required to maintain the operating temperature at constant values. Usually, heat is supplied directly to the electrolyzer and to the evaporator. The advantage of SOWE becomes determinant when heat sources (e.g. high-temperature nuclear reactors or concentrated solar power) are available. In this case, the formal conversion efficiency of electrical energy into thermal energy of hydrogen is about 1.3−1.4. On a less positive side, high operating temperatures and use of thin-walled ceramic solid electrolyte films create some problems. A very promising trend is to develop SOWE cells that can operate at significantly lower temperatures (e.g. 500−700 °C). However, solid electrolyte materials operating in this temperature range (e.g. Bi_2O_3)[43] lack stability and suffer from the onset of mixed (electronic + ionic) conductivity, which reduces the output current. Thus, high-temperature solid-oxide electrolysis cells are attractive from the standpoint of thermodynamics (the equilibrium potential difference is less than 1 V at 900 °C) and kinetics (low overvoltage, low levels of diffusion limitations). This type of electrolyzer does not require precious metal catalysts and is not sensitive to impurities in the feed water. However, the problem of structural materials and design for high temperature is not fully resolved, and the development process of these electrolyzers is quite slow. Synergies with SOFC are expecting to improve the situation.

2.4.5 Limitations, Recent Advances and Perspectives

Cell components in solid-oxide water electrolyzers are similar to those used in SOFC technology. There are also strong synergies in terms of perspectives. However, even though solid-oxide cells can be operated either in fuel cell or electrolysis modes, operation in electrolysis mode adds some specific challenges to the materials. In particular, corrosion issues (especially at the anode during oxygen evolution) due to the high operating temperature are critical. In state-of-the-art technology, the rate of performance degradation under high steam contents remains too high for practical applications. Degradation processes are further accelerated by the corrosion of interconnects. The purity of the feed steam is known to have a large influence on the degradation rate. Cell tightness is generally obtained using glass seals or vitro-ceramic seals that cannot survive thermal cycling. The degradation rate expressed in %/h or μV/h has become a key performance indicator for that technology, even more significant that the cell efficiency. Performance tests made on a five-cell stack operating at 800 °C and 0.3 A/cm^2 revealed a degradation rate of cell voltage close to 15%/1000 h.[44] The problem has been confirmed by the developments made at Ceramatec Co. (USA) and Idaho National Laboratory[45]: even at low current densities, a degradation rate close to 20%/1000 h has been observed at 800−900 °C. But improvements are being made. Results obtained in the course of the recent EU-FP7 RelHy project showed a degradation rate less than 5%/1000 h at 800 °C and 0.6 A/cm^2.[46] The exact nature of these degradation mechanisms is unknown and is asking for additional R&D.[47] It looks as if a compromise has to be found between performance and lifetime. Among various causes for performance degradation, the highly corrosive environment in the electrolyzer and mechanical and thermal constraints are responsible for most losses. Operation at lower temperatures (down to the 700−800 °C range) is expected to solve the problem. However, at such "low" temperatures, the ionic conductivity of best oxide-ion conductors (e.g. yttrium-stabilized ZrO_2) becomes insufficient. Some scandia-doped zirconium and some nickelates have been proposed[48] in replacement but there is a need for new solid materials. Finally, it should be mentioned that an interesting extension of steam electrolysis is the co-electrolysis of water vapor and carbon dioxide. It can be used to reduce steam contents in the feed gas and somewhat reduce corrosion issues. Also, it can improve the efficiency of the process and lead to the formation of a valuable syngas ($H_2 + CO$).[49]

2.5 CONCLUSION

Water electrolysis is a well-established technology that has been used for almost one century for miscellaneous application in the industry (food industry, power plants, metallurgy, etc.). Nowadays, it is also considered as a key process that can be used for the production of high-purity hydrogen from water and renewable energy sources. It is expected that in the near future, water electrolyzers will occupy an increasingly prominent place

for the decentralized production of hydrogen, for example, in hydrogen-fueling stations. Thus, in spite of its long industrial history, this is still the focus of several ambitious R&D programs and investments worldwide. There are different water electrolysis technologies. The difference between them comes from the temperature of operation and the pH of the electrolyte. The alkaline process is the oldest and a more mature one. But SPE water electrolysis has been making very significant progresses over the last years and because of its large potential for further improvement, it is expected to play a significant role in view of the so-called hydrogen economy and the large production of hydrogen of electrolytic grade from renewable energy sources. The high-temperature water electrolysis process is probably more efficient. However, it is faced with critical challenges (especially, in material science). Such challenges will have to be overcome before any market application can be considered.

References

1. Trasatti, S. Water Electrolysis: Who First? J. Electroanal. Chem. **1999**, *476*, 90–91.
2. Wetzels, Walter D. Johann Wilhelm Ritter: Romantic Physics in Germany In *Romanticism and the Sciences*; Cunningham, Andrew, Jardine, Nicholas, Eds.; Cambridge University Press: Cambridge; 1990, pp 199–212.
3. Fateev, V. N.; Porembsky, V. I.; Samoilov, D. I. *Electrochemical Method for Deuteroxide and Hydrogen Isotopes Producing in the Book "Isotopes"*; Fizmatlit: Moscow; 2005, 277–289.
4. Cerri, I. Lefebvre-Joud, F. Holtappels, P. Honegger, K. Stubos, T. Millet, P. In: Hydrogen and Fuel Cells', Scientific Assessment in support of the Materials Roadmap enabling Low Carbon Energy Technologies, JRC Scientific and Technical Reports, May 2012.
5. Sata, N. Proton Conduction in Mixed Perovskite-Type Oxides; Solid State Ionics **1999**, *125*, 383–387.
6. Kuleshov, N. V.; Korovin, N. V.; Terentyev, A. A.; Ryzhikov, A. V. Domestic Electrolysis—a Necessary Component of Hydrogen Energy in Russia. In *Proceedings of International Symposium of Hydrogen Energy. Moscow, November 1–2, 2005*; Publishing House of MPEI; pp. 156–162.
7. Rosa, V. M.; Santos, M. B. F.; Da Silva, E. P. New Materials for Water Electrolysis Diaphragms; Int. J. Hydrogen Energy **1995**, *20* (9), 697–700.
8. http://www.hydro.com.
9. http://www.hydrogenics.com.
10. http://www.teledynees.com.
11. http://www.uralhimmash.ru.
12. Divisek, J.; Murgen, J. Diaphragms for Alkaline Water Electrolysis and Method for Production of the Same as well as Utilization Thereof, U. S. Patent 4,394,244, 1983.
13. Pile, D.L.; Doughty, D.H.; Sandia National Laboratory, Report on DOE Contract DE-AC04-94AL85000 (2005).
14. Davenport, R. J.; Schubert, F. H. Space Water Electrolysis: Space Station through Advanced Missions; J. Power Sources **1991**, *36*, 235–250.
15. Mosdale, R.; Srinivasan, S. Analysis of Performance and of Water and Thermal Management in Proton Exchange Membrane Fuel Cells; Electrochim. Acta **1995**, *40* (4), 413–421.
16. Grigoriev, S. A.; Porembsky, V. I.; Fateev, V. N. Pure Hydrogen Production by PEM Electrolysis for Hydrogen Energy; Int. J. Hydrogen Energy **2006**, *31* (2), 171–175.
17. Timonov, A. M. Solid Polymer Electrolytes: Structure, Properties and Applications; Soros Educat. J. **2000**, *6* (8), 69–75.
18. Grubb, W.T. United States Patent No 2913511, 1959.
19. www2.dupont.com.
20. Kinumoto, T.; Inaba, M.; Nakayama, Y.; Ogata, K.; Umebayashi, R.; Tasaka, A.; Iriyama, Y.; Abe, T.; Ogumi, Z. Durability of Perfluorinated Ionomer Membrane Against Hydrogen Peroxide; J. Power Sources **2006**, *158*, 1222–1228.
21. Grigoriev, S. A.; Millet, P.; Fateev, V. N. Evaluation of Carbon-Supported Pt and Pd Nanoparticles for the Hydrogen Evolution Reaction in PEM Water Electrolysers; J. Power Sources **March 2008**, *177* (2), 281–285.
22. Grigoriev, S. A.; Khaliullin, M. M.; Kuleshov, N. V.; Fateev, V. N. Water Electrolysis in the System with a Solid Polymer Electrolyte; Russian J. Electrochemistry **2001**, *37* (8), 953–957.
23. http://www.hamiltonsundstrand.com.
24. http://www.protononsite.com.
25. http://www.yara.com.
26. http://www.h-tec.com.
27. Millet, P.; Andolfatto, F.; Durand, R. Design and Performance of a Solid Polymer Electrolyte Water Electrolyzer; Int. J. Hydrogen Energy **February 1996**, *21* (2), 87–93.
28. Yamaguchi, M.; Horiguchi, M.; Nakanori, T. Development of Large-Scale Water Electrolyzer Using Solid Polymer Electrolyte in WE-NET. *Proceedings of the 13th World Hydrogen Energy Conference*, Beijing, China, June 12–15, 2000, Vol. 1, pp. 274–281.
29. http://www.genhypem.u-psud.fr.
30. Fateev, V. N.; Archakov, O. V.; Lyutikova, E. K.; Kulikova, L. N.; Porembsky, V. I. Water Electrolysis in Systems with a Solid Polymer Electrolyte; Electrochemistry **1993**, 551–557; T. 29. P. 551. No 4.
31. Millet, P.; Ngameni, R.; Grigoriev, S. A.; Mbemba, N.; Brisset, F.; Ranjbari, A.; Etiévant, C. PEM Water Electrolyzers: from Electrocatalysis to Stack Development; Int. J. Hydrogen Energy **2010**, *35*, 5043–5052.
32. Dinh Nguyen, M-T.; Ranjbari, A.; Catala, L.; Brisset, F.; Millet, P.; Aukauloo, A. Implementing Molecular Catalysts for Hydrogen Production in Proton Exchange Membrane Water Electrolysers; Coord. Chem. Rev. **2012**, *256*, 2435–2444.
33. Grigoriev, S. A.; Millet, P.; Porembsky, V. I.; Fateev, V. N. Development and Preliminary Testing of a Unitized Regenerative Fuel Cell Based on PEM Technology; Int. J. Hydrogen Energy **March 2011**, *36* (6), 4164–4168.
34. Perfiliev, M. V.; Demin, A. K.; Kuzin, B. L.; Lipilin, A. *High-Temperature Gases Electrolysis*; Science: Moscow; 232.
35. Korobtsev, S.V. *Development of Fundamental Technologies of Production and Use of Hydrogen based on Solid Oxide Electrochemical Reversible High-Temperature Systems*; Report on Round-Table Meeting "Russian Research and Development in the Field of Hydrogen Technologies": Moscow, February 8, 2006.
36. Hauch, A.; Jensen, S.H.; Mogensen, M. Ni/YSZ Electrodes in Solid Oxide Electrolyzer cells, *Proceedings of the 26th Risø International Symposium on Materials Science: Solid State Electrochemistry*, Roskilde, Denmark, 2005, pp. 203–208.
37. O'Brien, J. E.; Stoots, C. M.; Herrings, J. S., et al. Hydrogen Production Performance of 10-Cell Planar Solid Oxide Electrolysis Stack; J. Fuel Cell Sci. Technol. **May, 2006**.
38. Quandt, K. H.; Streicher, R. Concept and Design of a 3.5 MW Pilot Plant for High Temperature Electrolysis of Water Vapor; Int. J. Hydrogen Energy **1985**, *11*, 309–315.

39. Mogensen, M.; Jensen, S.H.; Hauch, A.; Chorkendorff, I.; Jacobsen, T. *Proceedings 7th European SOFC Forum (2006)*, Lucerne, Switzerland, July 2008.
40. Stoots, C.; O'Brien, J.E.; Hawkes, G.L.; Herring, J.S.; Hartvigsen, J.J. High Temperature Steam and Carbon Dioxide Electrolysis Experiments at INL, Workshop on High Temperature Electrolysis, Roskilde, Denmark, September 18–19, 2006.
41. Jensen, S. H.; Larsen, P. H.; Mogensen, M. Hydrogen and Synthetic Fuel Production from Renewable Energy Sources; Int. J. Hydrogen Energy **2007**, *32*, 3253–3257.
42. Dyomin, A. K.; Kuzin, B. L.; Lipilin, A. S. A Pilot Study of a Thermal Mode of a High-Temperature Electrolyser for Water Decomposition; Electrochemistry **1987**, *23*, 1258–1260.
43. Zhuravlev, V.D.; Lobachevsky, N.I.; Bamburov, V.G.; Kozhevnikov, V.L. Investigation of the Conductivity of Solid Solutions based on Bi_2O_3, *The 8th International Workshop "Fundamental Problems of Solid Body Ionics*." Chernogolovka, 2006, p. 217.
44. Brisse, A.; Schefold, J.; Zahid, M. High Temperature Water Electrolysis in Solid Oxide Cells; Int. J. Hydrogen Energy **2008**, *33*, 5375–5382.
45. Herring, S.; O'Brien, J. E.; Stoots, C. M.; Hawkes, G. L.; Hartvigsen, J. J.; Shahnam, M. Progress in High Temperature Electrolysis for H_2 Production Using Planar SOFC Technology; Int. J. Hydrogen Energy **2007**, *32*, 440–450.
46. Schefold, J.; Brisse, A.; Zahid, M. *Proceeding of the 217th ECS Meeting*, Vancouver, Canada, April 25–30, 2010.
47. Sohal, S. *Manohar Degradation in Solid Oxide Cells During High Temperature Electrolysis*; Idaho 83415; Idaho National Laboratory: Idaho Falls; http://www.inl.gov; Prepared for the U.S. Department of Energy Office of Nuclear Energy Under DOE Idaho Operations Office Contract DE AC07-05ID14517.
48. Stevens, P.; Bassat, J-M.; Mauvy, F.; Grenier, J-C.; Lalanne, C. Matériaux d'anode pour SOEC, French Patent EDF/CNRS WO 2006/008390.
49. Zhan, Z.; Kobsiriphat, W.; Wilson, J. R.; Pillai, M.; Kim, I.; Barnett, S. A. Syngas Production by Coelectrolysis of CO_2/H_2O: The Basis for a Renewable Energy Cycle; Energy Fuels **2009**, *23*, 3089–3096.

This page intentionally left blank